Measurement of Asymmetric Optical Pumping of Ions Accelerating in a Magnetic-Field Gradient

Xuan Sun and Earl Scime
Department of Physics, West Virginia University, Morgantown, West Virginia 26506, USA

Mahmood Miah and Samuel Cohen
Princeton Plasma Physics Laboratory, Princeton, New Jersey 08543, USA

Frederick Skiff
Department of Physics and Astronomy, University of Iowa, Iowa City, Iowa 52242, USA
(Received 26 April 2004; revised manuscript received 26 August 2004; published 30 November 2004)

We report observations of asymmetric optical pumping of argon ions accelerating in a magnetic-field gradient. The signature is a difference in the laser-induced-fluorescence emission amplitude from a pair of Zeeman-split states. A model that reproduces the dependence of the asymmetry on magnetic-field and ion-velocity gradients is described. With the model, the fluorescence intensity ratio provides a new method of measuring ion collisionality. This phenomenon has implications for interpreting stellar plasma spectroscopy data which often exhibit unequal Zeeman state intensities.

DOI: 10.1103/PhysRevLett.93.235002 PACS numbers: 52.25.Os, 32.50.+d, 52.38.Dx, 52.70.Kz

In a laser-induced-fluorescence (LIF) measurement of the ion-velocity-space distribution function (IVDF) in a plasma, the frequency of a narrow-linewidth, tunable laser is scanned across an absorption line of an ion and fluorescent emission measured as a function of laser frequency [1]. The Zeeman effect due to a magnetic field creates several absorption lines between the initial lower and upper states; each Doppler-broadened line is pumped at slightly different frequencies by a particular polarization of the incident photons, i.e., linearly polarized π lines and circularly polarized $\sigma^{\pm}$ lines. In this Letter, we describe observations of up to a factor of 2.5 difference in the amplitude of the LIF signal from Zeeman sublevels pumped with right and left circularly polarized photons for argon ions accelerating along a weakening magnetic field. This effect should be considered in many situations, such as interpretation of resonant scattering observed in the solar corona [2,3]. In stellar coronas or in laboratory plasmas, the magnetic field and plasma velocity may change rapidly, strongly affecting the Stokes V spectrum (the wavelength dependent amplitude difference between Zeeman-split σ lines) [2] and its interpretation.

A tunable diode laser at 668.614 nm pumps an Ar II metastable level. The resulting 442.70 nm fluorescence is measured with a photomultiplier detector [4]. An LIF signal versus laser-frequency measurement allows the ion temperature to be determined from the linewidth, the bulk ion flow speed along the laser from the line shift, and the magnetic-field strength from the Zeeman splitting. The splitting of the Ar II absorption transition is composed of three separated line clusters (σ^+, π, σ^-) containing a total of 18 transitions [5].

Until now, the only way to determine plasma density with LIF (for plasmas in which Stark broadening is negligible) has been to relate the plasma density to the intensity of the emitted fluorescent light with an absolutely calibrated light-collection apparatus. In this work, we demonstrate that the asymmetry in the $\sigma^{\pm}$ LIF signals from Zeeman sublevels is a strong function of the ion collisionality and therefore an uncalibrated LIF system can provide remote measurements of the local plasma density for highly ionized plasmas.

The experiments were performed in the magnetic-nozzle-experiment (MNX) facility (Fig. 1). A 4-cm diameter, steady-state helicon plasma flows along a magnetic field formed by a Helmholtz-coil pair. The plasma exits the main discharge chamber through a coaxial 2-cm-i.d., 3-cm-thick magnetic-nozzle coil used to control the magnetic-field gradient and then flows through an electrically floating, 0.5-cm-diameter plasma-limiting aperture and into the expansion region (ER) [6]. At low neutral pressures, an electric double layer forms in the vicinity of the plasma-limiting aperture and accelerates the ions out of the source at supersonic velocities, along the weakening magnetic field, and into the ER [6–8]. The linearly polarized laser beam is passed through a quarter-wave plate to create either right or left circularly polarized light and then propagates along the plasma axis from the ER towards the source. Presented in Fig. 2 are LIF measurements obtained using both left and right circularly polarized light. In each measurement, a low-energy (LEP) ion population and a high-energy (HEP) ion population (kinetic energy $\sim$20 eV) are evident [6]. The LEP is the result of local ionization of neutral argon; the HEP consists of argon ions accelerated through the aperture. The amplitude of the σ^+ component in the HEP is $\sim$2 times higher than the σ^- component, yet the σ^+ and σ^- signal amplitudes for the locally produced LEP population are equal. The six Doppler-broadened compo-

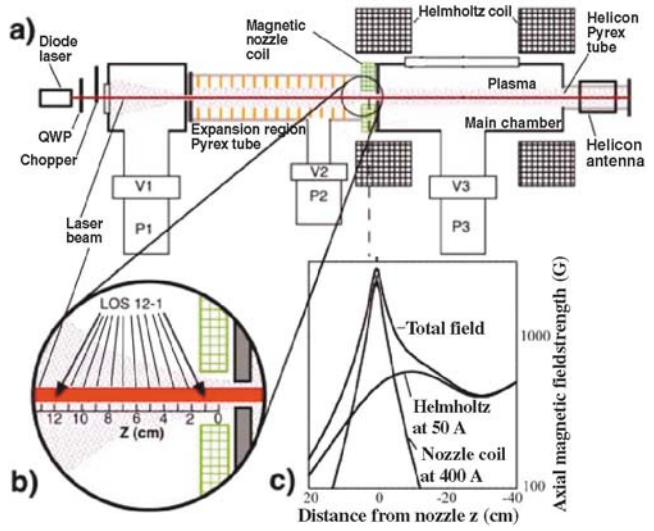

FIG. 1 (color). (a) Schematic of MNX. (b) Scanning mechanism for the LIF collection optics allows 12 line-of-sight (LOS) axial points in the ER. (c) Axial magnetic-field strength near the nozzle coil.

nents of each of the σ clusters are shown as vertical lines in Fig. 2, scaled according to their statistical weights [5].

As a function of the magnetic-nozzle field strength, B_N, the σ^+ and σ^- LIF signal amplitudes (A^+ and A^-, respectively) 2.9 cm downstream of the nozzle midplane ($z = 2.9$ cm) are shown in Fig. 3. The asymmetry ratio R, $R \equiv A^+/A^-$, increases with B_N to $R \sim 2.2$ at $B_N = 1700$ and then decreases slightly for larger values of B_N. $R > 1$ can arise from either enhanced absorption/fluorescence from the σ^+ ion LIF sequence or suppressed absorption/fluorescence from the σ^- sequence. In a recent study we demonstrated that, in helicon plasmas, the LIF intensity for Ar II is proportional to the square of the electron density times the square root of the electron temperature ($n_e^2 T_e^{0.5}$) [8]. The solid line in Fig. 3 is a linear fit to $n_e^2 T_e^{0.5}$

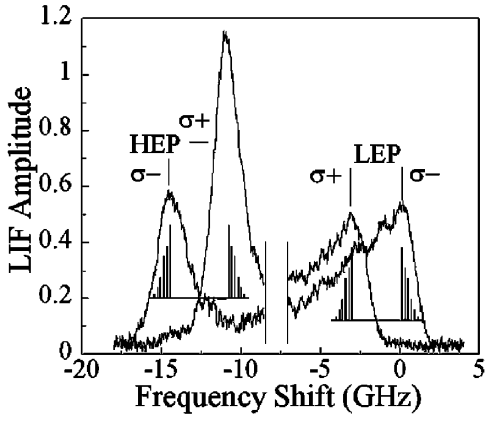

FIG. 2. LIF signal for right (σ^-) and left (σ^+) circularly polarized laser light versus the difference between laser frequency and natural frequency of the absorption line at $z = 2.9$ cm for $B_{\text{Helicon}} = 465$ G, $B_N = 1995$ G, $P = 550$ W, and neutral pressures of 0.6 mTorr and 0.23 mTorr in the source and ER, respectively.

measurements versus the nozzle field strength at $z = 7.0$ cm in the expansion region. That the scaling of the σ^+ LIF intensity versus the nozzle field strength is nearly identical to that of the $n_e^2 T_e^{0.5}$ measurements indicates that $R > 1$ arises because of a depletion of ions in the initial state of the σ^- sequence. Measurements at large values of B_N ($B_N = 2223$ G, and $P_M = 0.6$ mTorr) also indicate that the parallel ion kinetic energy increases from 13 eV at $z = 2$ cm to roughly 18 eV at $z = 7$ cm. Thus, as the ions move from a strong magnetic field in the nozzle coil to the weaker magnetic field in the ER, the σ^- states for the ions become less populated than the σ^+.

A number of possible explanations for the asymmetry in LIF intensities can be excluded. Creation of a spin-polarized beam by the longitudinal Stern-Gerlach effect [9] is implausible given the small ($\sim 1.0 \times 10^{-5}$ eV) energy splitting of these two σ clusters. The absence of any asymmetry in the LIF intensities from the σ clusters of the LEP ions rules out creation of a spin-polarized beam by the transverse Stern-Gerlach effect arising from the field gradients at the end of the solenoidal field. The magnetic-field strength-dependent Hanle effect can enhance the absorption of particular ion or atomic transitions. (In the Hanle effect, the energy of a Zeeman sublevel that increases with increasing magnetic-field strength can equal the energy of a Zeeman sublevel that decreases with magnetic field, thereby creating a degeneracy between the two states [10].) However, magnetic fields above 10 T would be required to obtain a level crossing between the initial state and the closest other ion states. Differences in the optical depth for the wavelengths corresponding to the peak of each of the σ clusters could also lead to an asymmetry in the LIF signal intensity. However, the measured absorption for each circular polarization over the length of the plasma was less than 1%. We also considered the Babcock procedure employed by stellar spectroscopists in which circularly polarized emission intensities from two thermally broadened, closely spaced, Zeeman-split σ lines are measured simultaneously at a wavelength slightly offset from the

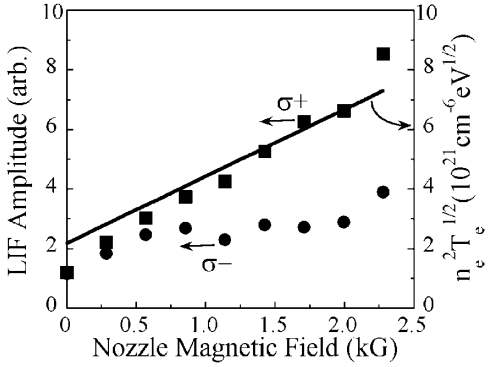

FIG. 3. The individual σ^+ and σ^- peak LIF amplitudes at $z = 2.9$ cm versus nozzle magnetic-field strength for $P = 580$ W, $B_H = 465$ G, and $P_M = 0.6$ mTorr.

unshifted line [11]. The difference in emission intensity is then directly proportional to the strength of the magnetic field. In our experiments the entire line shape of each Zeeman sublevel is measured and the peak intensities compared. Thus, although this effect gives a result similar to a Babcock-type measurement and could therefore be misinterpreted as evidence of a stronger than actual magnetic field in an astrophysical measurement, the physics responsible for the difference in signal intensities is not the same. We also note that the LIF intensity measurements presented here have been normalized to the instantaneous laser power and, to rule out any bias in the polarizing optics, the magnetic-field direction was reversed and the measurements repeated. For both directions of the magnetic field, the LIF signal of the higher frequency σ^+ HEP cluster was consistently larger than that of the σ^- HEP cluster, while those of the LEP stayed equal.

Other groups have demonstrated that saturation of an absorption line can begin at laser intensities comparable to those used in these experiments ($I \sim 1$ W/cm^2) [12]. We hypothesized that if the interaction time between the laser and the ions was different for ions in the initial σ^+ state compared to those in the initial state for the σ^- transition sequence, the LIF signal from the two transition sequences could differ. For example, if upstream of the observation volume ions in the initial σ^- state were in resonance with the laser for more time than ions in the initial σ^+, the population of σ^- state ions in the observation volume could be depleted, yielding a smaller LIF signal for that transition compared to the σ^+. Figure 4 presents a schematic view of how the resonant interaction times would differ for ions in different Zeeman-split states that accelerate through a magnetic-field gradient. The solid curve represents the decreasing magnetic field; the arrows indicate the direction of the ion velocity (and acceleration) and the laser-beam propagation. Close to the magnetic nozzle, the magnitude of the Zeeman shift of the σ lines relative to laser frequency at which the transition would appear in the absence of a static magnetic field (shown as a thick vertical line) is larger than further from the magnetic nozzle. Because the ions are accelerating towards the laser, the entire transition sequence shifts to a lower laboratory-frame frequency. Note that for measurements made at location b, when the laser is tuned to the peak of the σ^- line (dashed vertical line in Fig. 4), the σ^- state ions at the upstream location a are also pumped by the laser. Therefore, as the σ^- state ions travel along the laser- beam towards the measurement location their Zeeman and Doppler shifts can cancel—for appropriate velocity and field gradients—and the σ^- state ions are pumped by the laser for a much longer time than the σ^+ state ions.

Absorption out of the ith state is described by [12]

$$-\frac{d}{dt}N_i(z) = N_i(z)\frac{B_{ij}}{4\pi}\int_0^{+\infty} d\nu L_i(\nu)I(z, \nu, t), \quad (1)$$

where we have assumed that the HEP metastable ions are

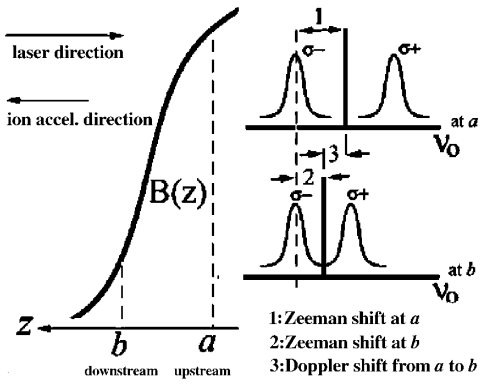

FIG. 4. Changes in absolute frequency of absorption lines due to Zeeman and Doppler shifts as ions accelerate through a magnetic-field gradient (solid curve).

created in the nozzle region by electron impact excitation of ground state ions and travel into the ER [6]. $N_i(z)$ is the density of the ith Zeeman sublevel of state $3d\,^4F_{7/2}$ at location z in the experiment. B_{ij} is the Einstein coefficient for absorption to the jth sublevel of the state $4p\,^4D_{5/2}$, where $j = i \pm 1$ for σ transitions. For B_{ij} we use the zero magnetic-field value, $B_{ij} \equiv E = 8.037 \times 10^{12}$ m^2 (Js)$^{-1}$. $I(z, \nu, t) = I_o\delta(\nu - \nu_o)$ is the laser intensity at frequency ν_o and $L_i(\nu) = (W_i/\sqrt{\pi\alpha_D T})\exp[-(\nu - \nu^*)^2/\alpha_D T]$ is the thermally broadened line shape of the ith Zeeman sublevel, where W_i is the statistical weight of the ith line, T the ion temperature, m_i the ion mass, and $\alpha_D = 2k_B\nu_o^2/m_ic^2$. In the laboratory frame, $\nu - \nu^* = \nu - [\nu_I + \alpha_iB(z)][1 - V(z)/c]$, where ν_I is the natural frequency of the absorption transition, α_i is the Zeeman shift for the ith sublevel [5], $B(z)$ is the magnetic field in kG, and $V(z)$ is the ion velocity. The factor of $1 - V(z)/c$ accounts for the Doppler shift of the line.

The length of time, t_r, before reaching the measurement location that ions may remain in resonance with the laser [13] is governed by the time between collisions for ions with background neutrals, electrons, and other ions: $t_r \equiv 1/\nu_i$, where ν_i is the total ion collision frequency. Rewriting Eq. (1) in terms of the travel distance of the

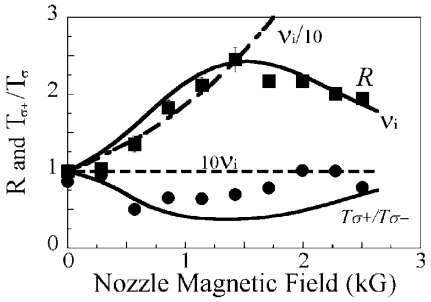

FIG. 5. Measured (solid squares) and predicted [solid (ν_i), dashed ($10\nu_i$), and dash-dotted line ($\nu_i/10$)] values of R versus B_N at $z = 2.9$ cm for $P = 750$ W, $B_H = 582$ G, and $P_M = 0.7$ mTorr. Also shown are the measured (solid circles) and predicted values (solid line) for $T_{\sigma^+}/T_{\sigma^-}$.

resonant ions, $\Delta z = V(z)/\nu_i$, yields the fraction of ions pumped out of the initial LIF state:

$$\frac{\Delta N_i(z)}{N_i} = \frac{E}{4\pi}\frac{W_i}{\sqrt{\pi\alpha_D T}}\int_{z-\Delta z}^{z}\frac{1}{V(z)}e^{-\{\nu_o-[\nu_I+\alpha_i B(z)][1-V(z)/c]\}^2/\alpha_D T}dz. \quad (2)$$

The LIF signal at z_o for a laser tuned to ν_o is proportional to the fluorescent emission due to laser pumping of the remaining fraction of initial state ions summed over the six sublevel transitions:

$$A^{\pm}(z_o) = \sum_{i=1}^{6} A_i^{\pm}(z_o) \propto \sum_{i=1}^{6}\left[\left(1-\frac{\Delta N_i(z_o)}{N_i}\right)M_i\int_0^{\infty} e^{-\{\nu-[\nu_I\pm\alpha_i B(z_o)][1-V(z_o)/c]\}^2/\alpha_D T} I_o\delta(\nu-\nu_o)d\nu\right]. \quad (3)$$

Eqation (3) describes the LIF intensity from σ^+ or σ^- ion states including any depletion of those states due to changing Zeeman and Doppler shifts for ions accelerating along the laser in a magnetic-field gradient before they reach the measurement location. Note that the ratio of A^+/A^- has no free parameters. To numerically integrate Eq. (3), we approximated the parallel ion flow and magnetic-field-strength gradients with fits to the measured ion flow and magnetic-field values: $V(z) = 267.2z + 7490\,\mathrm{m/s}$ and $B(z) = B_N[1 + (z/3.0)^2]^{-3/2}$ kG, with z in cm. The measured plasma parameters ($n_e = 7.5 \times 10^{10}$ cm^{-3}, $T_e = 6$ eV), ion temperature, $T_i = 0.2$ eV, and neutral pressure of 0.7 mTorr in the expansion region were used to calculate the limits of integration. For these parameters, the total ion collision frequency is dominated by the fast ion on background neutrals collision rate [14] and is independent of the electron temperature.

Measured and calculated values of R as a function of B_N are shown in Fig. 5 for the opposite magnetic-field orientation used to obtain the data of Fig. 3. The total ion collision frequency, based on the measured plasma parameters [14], is $\nu_i = 2.2 \times 10^5$ s^{-1}. R curves are shown for ν_i, $10\nu_i$, and $\nu_i/10$. Also shown in Fig. 5 are the measured and predicted parallel *inferred* ion temperature ratios ($T_{\sigma^+}/T_{\sigma^-}$) based on the HEP linewidths. The enhanced interaction of σ^- state ions with the laser distorts the measured parallel IVDF and affects the parallel ion temperature values obtained from Maxwellian fits. By varying the value of the laser frequency used in Eq. (3), a predicted IVDF measurement, and therefore a predicted value of $T_{\sigma^+}/T_{\sigma^-}$ is obtained. The predicted R values for the ion collision frequency based on the measured plasma parameters are in excellent agreement with the measurements. The dependence of $T_{\sigma^+}/T_{\sigma^-}$ on magnetic-nozzle field strength is generally consistent with the model predictions. The divergence between the measured and predicted values of $T_{\sigma^+}/T_{\sigma^-}$ above 1 kG is due to difficulties in fitting the highly asymmetric distributions predicted by the model for large B_N. The peak in R at a specific value of B_N is accurately reproduced by the numerical calculations (at large B_N the Doppler and Zeeman shifts are no longer commensurate). Factor of 10 variations in ν_i yield predicted R values that are clearly at odds with the measurements. The measured dependence of R on z (not shown) also agrees with the model; e.g., $R > 1$ and R increases with the distance from the aperture as the effects of the field and velocity gradients increase. When the ion acceleration region did not overlap with the magnetic-field gradient (accomplished by moving the aperture), $R = 1$ was observed in all cases.

Asymmetry in LIF emission from σ states of argon ions was observed and attributed to the combined effects of magnetic-field and ion-velocity gradients. This phenomenon should be considered in laboratory and stellar plasmas where, for example, turbulence can generate the requisite gradients. In stellar plasmas, the intensities of Zeeman-split absorption lines in ions accelerating away from the surface of stars, illuminated by continuum radiation from the photosphere, frequently exhibit similar asymmetries [2,3]. With the model described here, such measurements could provide additional information about the plasma conditions in those stellar atmospheres. Additionally, an uncalibrated LIF system can provide a noninvasive measurement of ν_i, and therefore the plasma density, in highly ionized plasmas.

This work was supported by U.S. Department of Energy Contract No. DE-AC02-76-CHO- 3073 and by EPSCoR Laboratory Partnership Program Grant No. ER45849.

[1] R. A. Stern and J. A. Johnson III, Phys. Rev. Lett. **34**, 1548 (1975).
[2] M. Sigwarth, Astrophys. J. **563**, 1031 (2001).
[3] H. Lin, M. Penn, and S. Tomczyk, Astrophys. J. **541**, L83 (2000).
[4] R. F. Boivin and E. E. Scime, Rev. Sci. Instrum. **74**, 4352 (2003).
[5] G. Marr, *Plasma Spectroscopy* (Elsevier, New York, 1968).
[6] S. A. Cohen *et al.*, Phys. Plasmas **10**, 2593 (2003).
[7] C. Charles and R.W. Boswell, Appl. Phys. Lett. **82**, 1356 (2003).
[8] X. Sun *et al.*, Plasma Sources Sci. Technol. **13**, 359 (2004).
[9] H. Batelaan, T. J. Gay, and J. J. Schwendiman, Phys. Rev. Lett. **79**, 4517 (1997).
[10] V. F. Weisskopf, Ann. Phys. (Leipzig) **9**, 23 (1931).
[11] H.W. Babcock, Astrophys. J. **118**, 387 (1953).
[12] M. J. Geockner and J. Goree, J. Vac. Sci. Technol. A **7**, 977 (1989).
[13] F. Skiff and J. J. Curry, Rev. Sci. Instrum. **66**, 629 (1995).
[14] A.V. Phelps, J. Phys. Chem. Ref. Data **20**, 557 (1991).